Full length article

NF-κB decoy oligodeoxynucleotide mitigates wear particle-associated bone loss in the murine continuous infusion model

Tzu-hua Lin [a], Jukka Pajarinen [a], Taishi Sato [a], Florence Loi [a], Changchun Fan [a], Luis A. Córdova [a,c], Akira Nabeshima [a], Emmanuel Gibon [a,d], Ruth Zhang [a], Zhenyu Yao [a], Stuart B. Goodman [a,b,∗]

[a] Department of Orthopaedic Surgery, Stanford University, Stanford, CA, USA
[b] Department of Bioengineering, Stanford University, Stanford, CA, USA
[c] Department of Oral and Maxillofacial Surgery, Faculty of Dentistry, University of Chile—CONICYT, Santiago, Chile
[d] Biomechanics and Bone & Joint Biomaterials Laboratory, UMR CNRS 7052, School of Medicine, Paris 7 University, Paris, France

ABSTRACT

Total joint replacement is a cost-effective surgical procedure for patients with end-stage arthritis. Wear particle-induced chronic inflammation is associated with the development of periprosthetic osteolysis. Modulation of NF-κB signaling in macrophages, osteoclasts, and mesenchymal stem cells could potentially mitigate this disease. In the current study, we examined the effects of local delivery of decoy NF-κB oligo-deoxynucleotide (ODN) on wear particle-induced bone loss in a murine continuous femoral particle infusion model. Ultra-high molecular weight polyethylene particles (UHMWPE) with or without lipopolysaccharide (LPS) were infused via osmotic pumps into hollow titanium rods placed in the distal femur of mice for 4 weeks. Particle-induced bone loss was evaluated by μCT, and immunohistochemical analysis of sections from the femur. Particle infusion alone resulted in reduced bone mineral density and trabecular bone volume fraction in the distal femur. The decoy ODN reversed the particle-associated bone volume fraction loss around the implant, irrespective of the presence of LPS. Particle-infusion with LPS increased bone mineral density in the distal femur compared with particle-infusion alone. NF-κB decoy ODN reversed or further increased the bone mineral density in the femur (3–6 mm from the distal end) exposed to particles alone or particles plus LPS. NF-κB decoy ODN also inhibited macrophage infiltration and osteoclast number, but had no significant effects on osteoblast numbers in femurs exposed to wear particles and LPS. Our study suggests that targeting NF-κB activity via local delivery of decoy ODN has great potential to mitigate wear particle-induced osteolysis.

Statement of Significance

Total joint replacement is a cost-effective surgical procedure for patients with end-stage arthritis. Chronic inflammation is crucial for the development of wear particle-associated bone loss. Modulation of NF-κB signaling in macrophages (pro-inflammatory cells), osteoclasts (bone-resorbing cells), and osteoblasts (bone-forming cells) could potentially mitigate this disease. Here we demonstrated that local delivery of decoy NF-κB oligo-deoxynucleotide (ODN) mitigated ultra-high molecular weight polyethylene (UHMWPE) wear particle induced bone loss in a clinically relevant murine model. The protective effects of decoy ODN was associated with reduced macrophage infiltration and osteoclast activation, but had no significant effects on osteoblast numbers. Our study suggests that targeting NF-κB activity via local delivery of decoy ODN has great potential to mitigate wear particle-induced bone loss.

1. Introduction

Total joint replacement (TJR) is a cost-effective surgical procedure for end-stage arthritis. Wear particles generated from implanted joint replacements are often associated with significant bone loss (periprosthetic osteolysis), which may lead to revision

∗ Corresponding author at: Department of Orthopaedic Surgery, Stanford University School of Medicine, 450 Broadway Street, Redwood City, CA 94063, USA.
E-mail address: goodbone@stanford.edu (S.B. Goodman).

surgery [1,2]. The revision procedure is technically difficult with higher complication rates; furthermore the total number of cases is increasing due to the aging society and the fact that TJR has been extended to younger patients.

Macrophages recognize wear particles or adherent endo- or exogenous danger signal molecules (such as endotoxin) via surface receptors including toll-like receptors (TLR), and can phagocytose smaller particles less than about 10 μm [3,4]. These processes lead to the activation of multiple signaling pathways including NF-κB [5]. The activated macrophages secrete many pro-inflammatory cytokines and chemokines and attract the infiltration of more immune cells and osteoclast progenitors [6,7]. Exposure of mesenchymal stem cells (MSCs) to wear particles interferes with cell viability and osteogenesis through an NF-κB dependent pathway [8]. Together, this suggests the great potential of NF-κB as a therapeutic target to mitigate wear particle-associated bone loss.

NF-κB is a master regulator of inflammation and bone remodeling [9]. Modulation of NF-κB activity has been applied to immune-related diseases in clinical trials [10]. Our recent studies have demonstrated that application of NF-κB decoy oligodeoxynucleotide (ODN), a synthesized duplex DNA that suppresses NF-κB activity through competitive binding [11], has promising effects to mitigate periprosthetic osteolysis using in vitro and in vivo models [8,12,13]. In primary mouse macrophages and the human macrophage cell line THP1, NF-κB decoy ODN simultaneously suppressed the secretion of multiple pro-inflammatory cytokines (TNF-α, IL-1β, and IL-6, etc.) and chemokines (MCP1, MIP1α, etc.) when cells were exposed to ultra-high molecular weight polyethylene (UHMWPE) particles [12]. In primary mouse and human mesenchymal stem cells (MSCs), NF-κB decoy ODN protected cell viability and osteogenic differentiation ability when exposed to UHMWPE particles [8]. In addition, the ratio of receptor activator of NF-κB ligand (RANKL)/osteoprotegerin (OPG) secreted by MSCs was also reduced by the decoy ODN, which may suppress osteoclast activation through paracrine regulation [14].

NF-κB decoy ODN was also shown to increase bone mineral density in mouse calvaria exposed to a single application of UHMWPE particles [13]. Furthermore, macrophage infiltration and osteoclast activation were decreased in the mice treated with the decoy ODN. The mouse calvarial model is a valuable short-term screening model that uses a single application of particles onto a flat bone; however, this model may not fully reflect the clinical timeline or biological processes of continuous particle delivery into a long bone as it occurs in lower limb joint replacement.

For this reason, we examined the effects of NF-κB decoy ODN in a continuous murine femoral infusion model [15] using clinically relevant UHMWPE particles. Endotoxin was also included in some of the groups as a model of danger-signal molecules adhering to the particles. The particles and decoy ODN were slowly released into the distal femur using implanted osmotic pumps, which mimics the continuous production of wear particles in TJR patients. Our results indicate that local delivery of NF-κB decoy ODN can mitigate the inflammatory response and bone loss in a clinical translational model of wear particle-associated periprosthetic osteolysis.

2. Materials and methods

2.1. Decoy oligodeoxynucleotide

The NF-κB decoy ODN sequences used are 5′-CCTTGAAGG GATTTCCCTCC-3′ and 3′-GGAACTTCCCTAAAGGGAGG-5′. Scrambled ODN sequences are 5′-TTGCCGTACCTGACTTAGCC-3′ and 3′-AACGG CATGGACTGAATCGG-3′ [16]. The ODNs were synthesized by Integrated DNA Technologies (IDT, Coralville, IA, USA) in HPLC grade.

2.2. Ultra-high molecular weight polyethylene particles

Conventional UHMWPE particles were a gift from Dr. Timothy Wright (Hospital for Special Surgery, New York) and obtained from knee joint simulator tests and isolated according to an established protocol [17]. Frozen aliquots of the particles containing serum were lyophilized for 4–7 days. The dried material was digested in 5 M sodium hydroxide at 60 °C for 1 h, and ultrasonicated for 10 min. The digested particle suspension was centrifuged through a 5% sucrose gradient at 40 K rpm at 10 °C for 3 h. The collected particles at the surface of the sucrose solution were incubated at 80 °C for 1 h and centrifuged again through an isopropanol gradient (0.96 and 0.90 g/cm³) at 40 K rpm at 10 °C for 1 h. The purified particles at the interface between the two layers of isopropanol were harvested and the isopropanol was evaporated from the particle mixture then lyophilized until dry. Particles were then re-suspended in 95% ethanol, which was evaporated completely. The particles tested negative for endotoxin using a Limulus Amebocyte Lysate Kit (BioWhittaker, Walkersville, MD). The mean diameter of the particles was 0.48 ± 0.10 μm (mean ± SE, averaged from 125 scanned particles ranged from 0.26 μm to 0.81 μm) measured by electron microscopy. The measurement was done by Dr. Lydia-Marie Joubert in the Cell Science Image Facility at Stanford University.

2.3. In vitro osmotic pump releasing model

The mouse macrophage cell line RAW 264.7 cells (Cat. TIB-71, ATCC, Manassas, VA) stably expressing luciferase driven by NF-κB response elements were generated as previously described [12]. The cells were grown in Dulbecco's Modified Eagle Medium (DMEM) supplemented with 10% Fetal Bovine Serum (FBS) and an antibiotic/antimycotic solution (100 units of penicillin, 100 μg of streptomycin, and 0.25 μg of Amphotericin B per ml; Hyclone, Thermo Scientific). Eight Alzet mini-osmotic pumps (Model 2006) with a mean flow rate of 0.15 μl/hour were connected via 6 cm vinyl tubing (Durect Corporation) to a collection eppendorf filled with 500 μl RAW 264.7 cell culture media as previously described [18]. The pumps were filled with UHMWPE particles (15 mg/ml), together with decoy or scrambled ODN (50 μM, 4 independent pump-set per group). The conditioned media were collected weekly (week 1, 2, 3, and 4). The amounts of ODN were quantified by Picogreen assay (ThermoFisher Scientific, Waltham, MA). To confirm the sustained biological activity of the released ODN, RAW 264.7 reporter cells were treated with collected media supplemented with 1 μg/ml Lipopolysaccharide (LPS, purchased from Sigma-Aldrich St. Louis, MO) for 24 h. The luciferase activity was determined by using the luciferase assay system (Promega, Madison, WI) and read by a Luminometer (Turner Biosystem, Sunnyvale, CA) or IVIS-200 (Perkin Elmer, Santa Clara, CA). The secretion of tumor necrosis factor-α (TNF-α) was quantified using a mouse TNF-α colorimetric ELISA kit (R&D Systems).

2.4. Continuous femoral infusion murine model

Male athymic nude mice (Charles River), 10–15 weeks of age were used for the experiments (9–11 mice per group). The animal protocol was approved by the institutional ethics committee. Institutional guidelines for the care and use of laboratory animals were observed in all aspects of this project. Alzet mini-osmotic pumps (Model 2006) were connected to vinyl tubing and a hollow titanium rod placed in the distal femur through the intercondylar region. The pumps were filled with various combinations of UHMWPE particles (15 mg/ml), decoy ODN (50 μM), and/or LPS (1 μg/ml) as: (1) untreated control, (2) particle infusion alone, (3) particle infusion with decoy ODN, (4) particle infusion with

scrambled ODN, (5) particle infusion with LPS, (6) particle infusion with LPS and decoy ODN, and (7) particle infusion with LPS and scrambled ODN.

2.5. Micro-computational tomography (μCT)

The mice underwent μCT scans at Day 0 (before surgery) and Day 28 (after sacrifice and removal of the titanium rod) using a GEHC μCT scanner with 49 μm resolution (GE Healthcare, Fairfield, CT). The 3D re-constructed images were created from the region of interest (ROI) in the trabecular bone region (40 slices between 1 and 3 mm from distal end of femur) generated by advanced 3D spline tool. Bone volume fraction (BVF, data presented as the ratio of bone volume/total volume) in the trabecular bone region was determined in ROI near the end of titanium rod (20 slices between 2 and 3 mm from distal end of femur). The ROI (4 mm × 4 mm × 3 mm) at the metaphysis site was created within the distal part of the femur which began 3 mm from the distal end of the femur and proceeded proximally. The ROI at the diaphysis site (4 mm × 4 mm × 3 mm) was created beginning from the end of the metaphysis and proceeding proximally. The threshold bone mineral density (BMD, data presented in unit of mg/ml) was quantified by GEMS MicroView (threshold: 700 HU).

2.6. Tissue processing and histology

The femurs from operated and non-operated sites were excised after μCT scanning. The rod was removed to allow for thin sectioning and immunohistochemical analysis. Femurs were fixed in 4% paraformaldehyde overnight, and decalcified in 0.5 M ethylenediamine tetra acetic acid (EDTA, pH 7.9) for 2 weeks. The specimens were embedded in optimal cutting temperature (OCT) compounds and the ROI between 2 and 3 mm (Fig. 2b) from the distal end of femur was cut into 10 μm transverse sections for subsequent staining. Hematoxylin and Eosin (H&E) staining was performed for histological analysis.

2.7. Immunohistochemistry and cell counting

Macrophages were detected by immunofluorescence staining using PE-conjugated anti-CD11b antibody (BD, Franklin Lake, NJ). Rat IgG2b-PE antibodies were used as isotype control. The slides were mounted with ProLong Gold Antifade Mount with DAPI (Life Technologies, Grand Island, NY). CD11b+ cells were manually counted under a fluorescence microscope (Axio Observer 3.1, Zeiss, Oberkochen, Germany) in 3 randomly selected fields of view. Osteoblasts and osteoclasts were determined as previously described [13]. In brief, osteoblasts were identified by anti-alkaline phosphatase (ALP) antibody (R&D, Minneapolis, MN) with the use of Avidin-biotin complex (Vector Laboratories) immunohistochemistry. The positively-stained cells were counted manually and normalized by total lengths of periosteum and endosteum quantified by Image J software. Osteoclast-like cells were determined by leukocyte tartrate resistant acid phosphatase (TRAP) staining kit (Sigma Aldrich) with multi-nucleated cells located on the bone perimeter within the resorption lacunae. The stained-positive cells were counted manually and normalized by total bone area quantified by Image J (software, National Institutes of Health, USA).

2.8. Statistical analysis

Unpaired Student's t tests were performed using the data of the luciferase activity assay and ELISA assay for the in vitro studies. Two-way ANOVA with Holm-Sidak multiple comparison test was performed for the in vitro pump releasing experiments. One-way ANOVA with Tukey's post-hoc test was performed to quantify the results of μCT scanning and immunohistochemistry staining. The statistical analysis was conducted using Prism 5 (GraphPad Software, San Diego, CA). Data were reported as mean ± standard error of the mean. P < 0.05 was chosen as the threshold of significance.

3. Results

3.1. Functional assessment of NF-κB decoy ODN released by osmotic pumps in an in vitro model

Although the in vitro effects of the decoy ODN on macrophages were characterized in our previous study [12], an in vitro experiment was carried out similar to one previously described [18] to assess the stability of the NF-κB decoy ODN during long term release from osmotic pumps (Fig. 1a). The amounts of NF-κB or scrambled ODNs showed no significant difference among the samples collected over the timespan of 4 weeks as quantified by the PicoGreen assay (Fig. 1b). The NF-κB activity in RAW264.7 reporter cells was significantly suppressed by the NF-κB decoy ODN collected at all the time points (Fig. 1c). Suppression of NF-κB activities in collected decoy ODNs during the first week translated to reduction of TNF-α secretion in LPS stimulated RAW264.7 cells (Fig. 1d). We noticed that the level of reduced TNF-α was not as clear as the reduced NF-κB activity. The results were confirmed by using fresh decoy ODN with the same experimental conditions. The concentration of the ODN (5 μM) was determined by estimating pump releasing rate. The results showed that the inhibition of NF-κB activity and TNF-α secretion by the fresh decoy ODN paralleled the results of the samples collected at week 1 (Fig. 1e). These results suggested the expression of TNF-α in RAW264.7 exposed to the wear particles and LPS involved multiple signaling pathways [19].

3.2. NF-κB decoy ODN mitigated UHMWPE wear particle-associated trabecular bone loss in a murine femoral continuous particle infusion model

The continuous particle infusion model was then used to investigate the ability of NF-κB decoy ODN to mitigate wear particle-associated osteolysis in vivo (Fig. 2a). The 3D images in the trabecular bone region affected by UHMWPE wear particle infusion (between 1 and 3 mm from distal end of femur) were generated to evaluate the therapeutic potential of the decoy ODN (Fig. 2b and c upper panel). Infusion of UHMWPE particles alone or combined with LPS significantly reduced the amount of trabecular bone around the end of the titanium rod where particles were released (indicated by yellow lines). No statistical significant difference was observed between the group of particle alone or combined with LPS (p = 0.12). NF-κB decoy ODN, but not scrambled ODN, mitigated the particle-associated bone loss. The phenomenon was confirmed in 2D transverse images and histological sections from the same area (Fig. 2b and c middle and bottom panels). Quantification of BVF in the ROI1 (see Fig. 3a) in trabecular bone (between 2 and 3 mm from distal end of femur) confirmed that particle-infusion with or without LPS (0.23 ± 0.03 and 0.36 ± 0.02, respectively, compared with untreated control group at 0.47 ± 0.03) induced significant trabecular bone loss, whereas NF-κB decoy ODN mitigated these effects (0.49 ± 0.04 and 0.50 ± 0.05, respectively, Fig. 2d). Particle infusion with LPS showed a tendency for reduction in BVF compared with particles alone (p = 0.08), but the tendency was not observed in decoy or scrambled ODN treated groups. Particle-infusion with LPS and scrambled ODN increased the BVF to 0.34 ± 0.04 compared to the control group without ODN, but it did not reach statistical significance (p = 0.15).
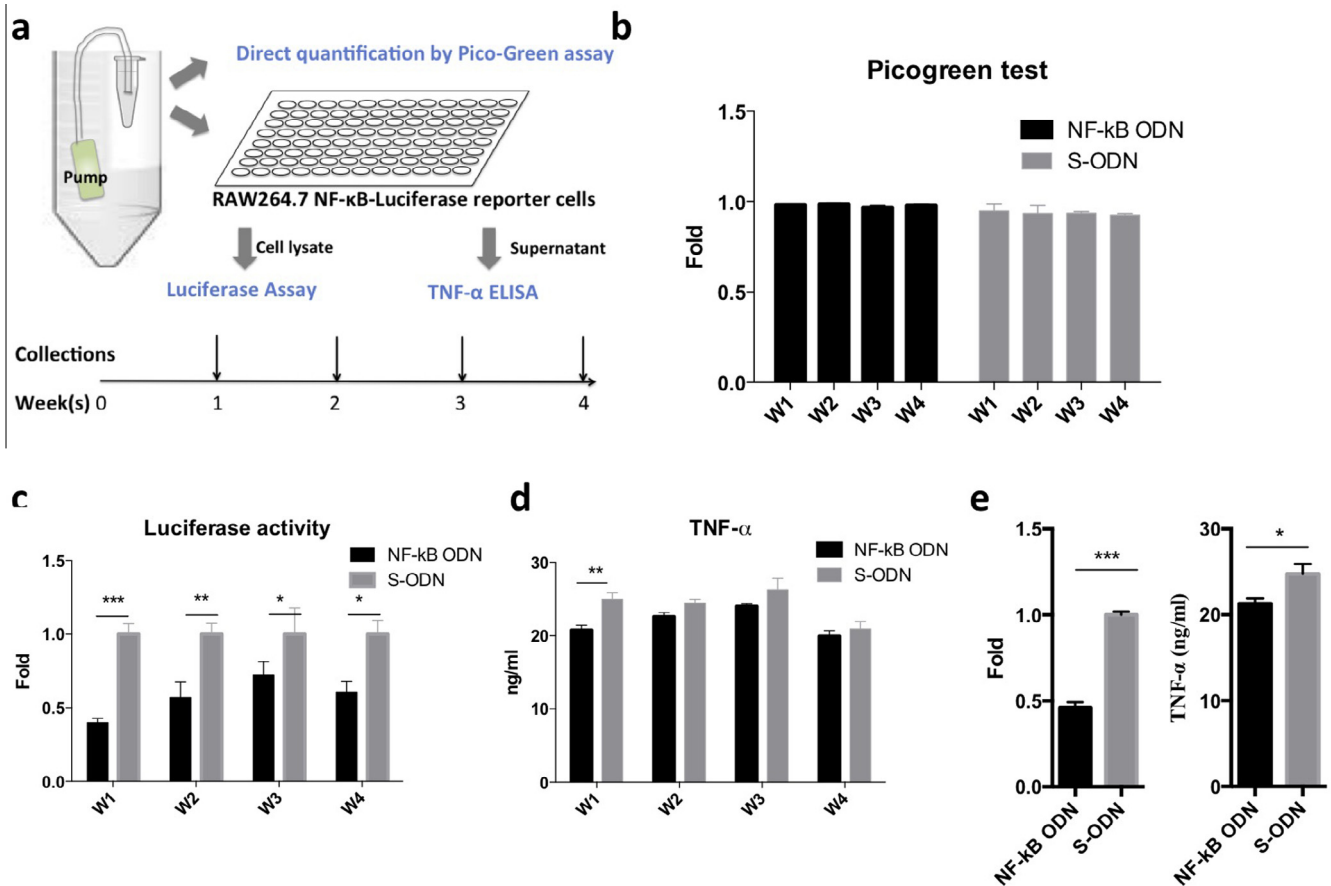
Fig. 1. NF-κB decoy ODN released from osmotic pumps inhibited NF-κB activity induced by LPS in RAW264.7 reporter cells. (a) Illustration of in vitro osmotic pump releasing model. The osmotic pumps were filled with UHMWPE particles (15 mg/ml) and NF-κB decoy ODN or scrambled ODN (50 µM) to mimic the in vivo murine model. The released ODNs in culture media were collected weekly for 4 weeks, and the amounts of ODNs were quantified by Picogreen assay (b). RAW264.7 NF-κB reporter cells were exposed to the conditioned media and LPS (1 µg/ml) for 24hrs. The cells were lysed for luciferase assay to quantify the NF-κB activities (c). Cellular supernatants were collected to measure the secreted TNF-α by ELISA (d). The fresh decoy ODN (5 µM) was applied to quantify the inhibition effects of NF-κB activity and TNF-α secretion in RAW264.7 reporter cells exposed to LPS and UHMWPE particles (e). S-ODN: scrambled ODN; PE: UHMWPE. *p < 0.05, **p < 0.01, ***p < 0.005.

3.3. NF-κB decoy ODN mitigated UHMWPE wear particle-associated reduction of bone mineral density in the diaphyseal region

The particles were released at the end of metaphyseal region, and it was anticipated that the particles would further diffuse to the diaphysis region through the bone marrow cavity. ROI ($4 \times 4 \times 3 \text{ mm}^3$) containing metaphyseal (ROI2) or diaphyseal (ROI3, Fig. 3a) regions were generated to analyze the effects on BMD by particle and decoy ODN infusion. The alterations of BMD (aBMD) were normalized by the values determined in the pre-operative scans as described in Section 2. In the metaphyseal region (Fig. 3b), UHMWPE particle infusion significantly reduced aBMD from 15.98 ± 6.82 mg/ml to −32.34 ± 8.34 mg/ml, while the values for treatment with decoy ODN and scrambled ODN in particle-infused mice were −33.58 ± 6.36 and −60.76 ± 10.91 mg/ml, respectively. Infusion of UHMWPE particles plus LPS significantly increased aBMD to 13.18 ± 8.65 mg/ml when compared with the particle alone group, which could be correlated with increased trabecular bone in the distal end of the femur observed in the 3D images (Fig. 2c). When combined treatment with decoy ODN was examined, aBMD was significantly increased to 44.72 ± 8.63 mg/ml. In the diaphyseal region (ROI3), particle infusion alone (32.41 ± 6.85 mg/ml) significantly reduced aBMD when compared with the untreated control (75.80 ± 9.69 mg/ml, Fig. 3d). Infusion of particles plus LPS increased the value of BMD to 61.89 ± 10.18 mg/ml, which is similar to the observation in the metaphyseal region. Decoy ODN

(69.36 ± 7.06 mg/ml), but not scrambled ODN (32.89 ± 9.60 mg/ml), reversed the bone loss effect in the particle alone group, and further increased aBMD in the particles plus LPS treated group (109.50 ± 11.87 mg/ml). Infusion of UHMWPE particles and LPS showed similar effects on aBMD in the non-operated contralateral femurs at both metaphysis and diaphysis regions (Fig. 3c and e), which is consistent with our previous reports of systemic effects [20]. The systemic effects of decoy ODN on contralateral femurs did not reach to statistical significance (Fig. 3c and e).

3.4. NF-κB decoy ODN reduced macrophage infiltration induced by UHMWPE wear particles with LPS

The number of macrophages in the transverse sections was determined by CD11b immunofluorescence staining (Fig. 4). CD11b+ cells were increased in the group with particle infusion (12.56 ± 1.82 cells/view) or combined with LPS (31.37 ± 4.06 cells/view) compared to the untreated control group (1.44 ± 0.47 cells/view). Decoy ODN reduced CD11b + cell number in the particle plus LPS group (17.63 ± 3.23 cells/view), and showed a tendency for reduction in particle alone group (8.71 ± 1.63 cells/view, p = 0.15). The CD11b + cell numbers in the scrambled ODN group were comparable to the control groups with particle infusion alone (12.38 ± 1.81 cells/view) or particle plus LPS (30.00 ± 3.24 cells/view), respectively.
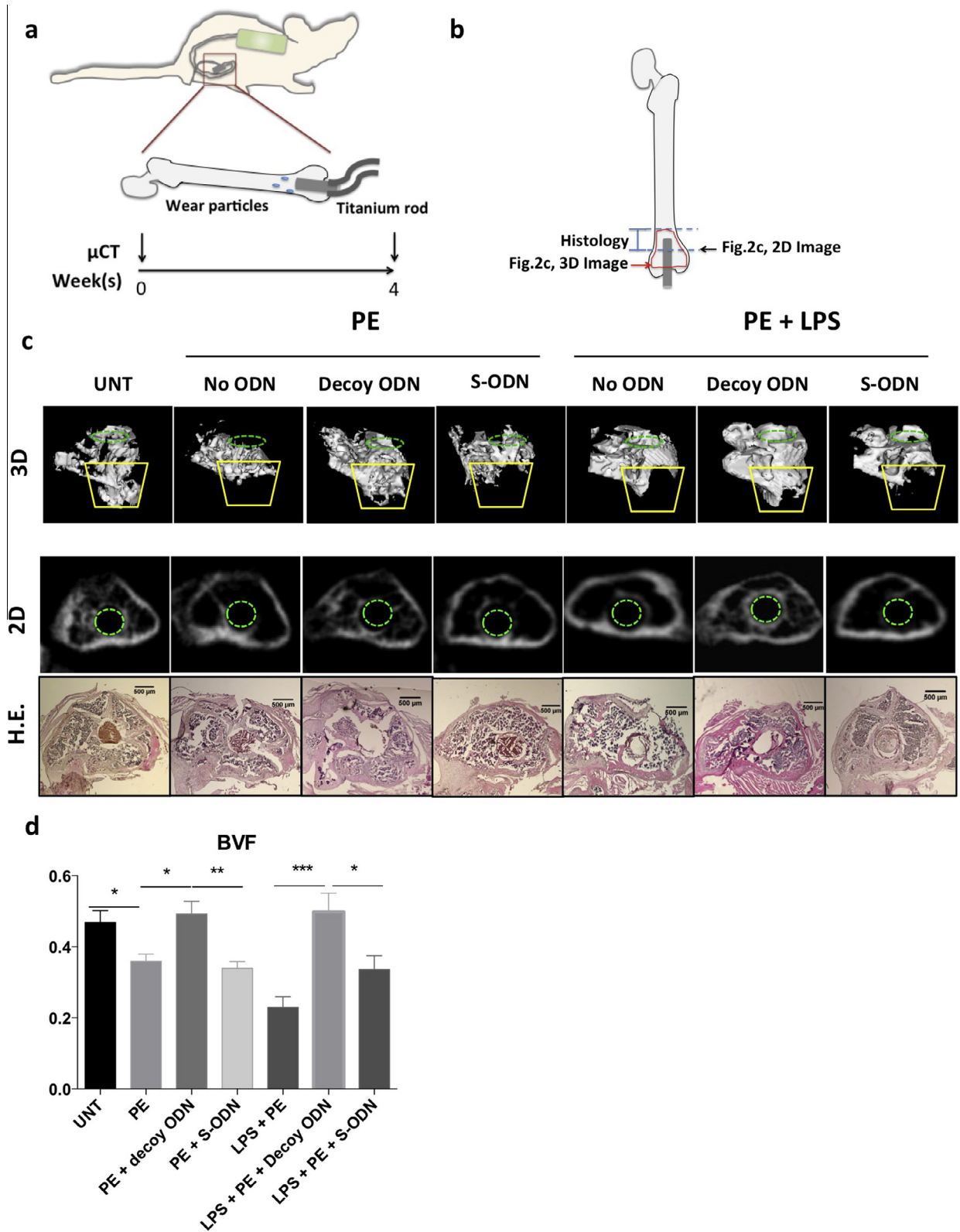
Fig. 2. NF-κB decoy ODN mitigated bone loss in murine femurs during continuous UHMWPE wear particle infusion. (a) Illustration of in vivo murine model with continuous femoral infusion. Mouse distal femur were exposed to saline control or UHMWPE particles together with 50 μM decoy ODN or scrambled ODN, with or without 1 μg/ml LPS for 4 weeks. μCT scanning was performed 1 day before and 4 weeks after the operation. (b) Illustration of ROI used for image analysis. (c) Trabecular bone structures in the distal femur were reconstructed into a 3D image. ROI was generated by selecting the region inside cortical bone on 2D image for every 10th slice for 5 sections (from 1 mm to 3 mm from the distal femur). Yellow lines indicate the major bone loss area induced by UHMWPE particles with/without LPS infusion (ROI1, see Fig. 3a for details). Green dotted circle (in 3D and 2D image) indicated the inserted titanium rod channel from intercondylar region at distal femur. The 2D image (*middle*) and H&E histology staining (*bottom*) around 2.5 mm from distal femur were consistent with the observation in 3D image (*upper*). (d) BVF (700–2000 HU) in the ROI1 including the major bone loss observed in the 3D image (from 2 mm to 3 mm from the distal femur in trabecular bone region) were quantified by MicroView Software. PE: UHMWPE particles; UNT: untreated control; S-ODN: scrambled ODN. $^*p < 0.05$, $^{**}p < 0.01$, $^{***}p < 0.005$.
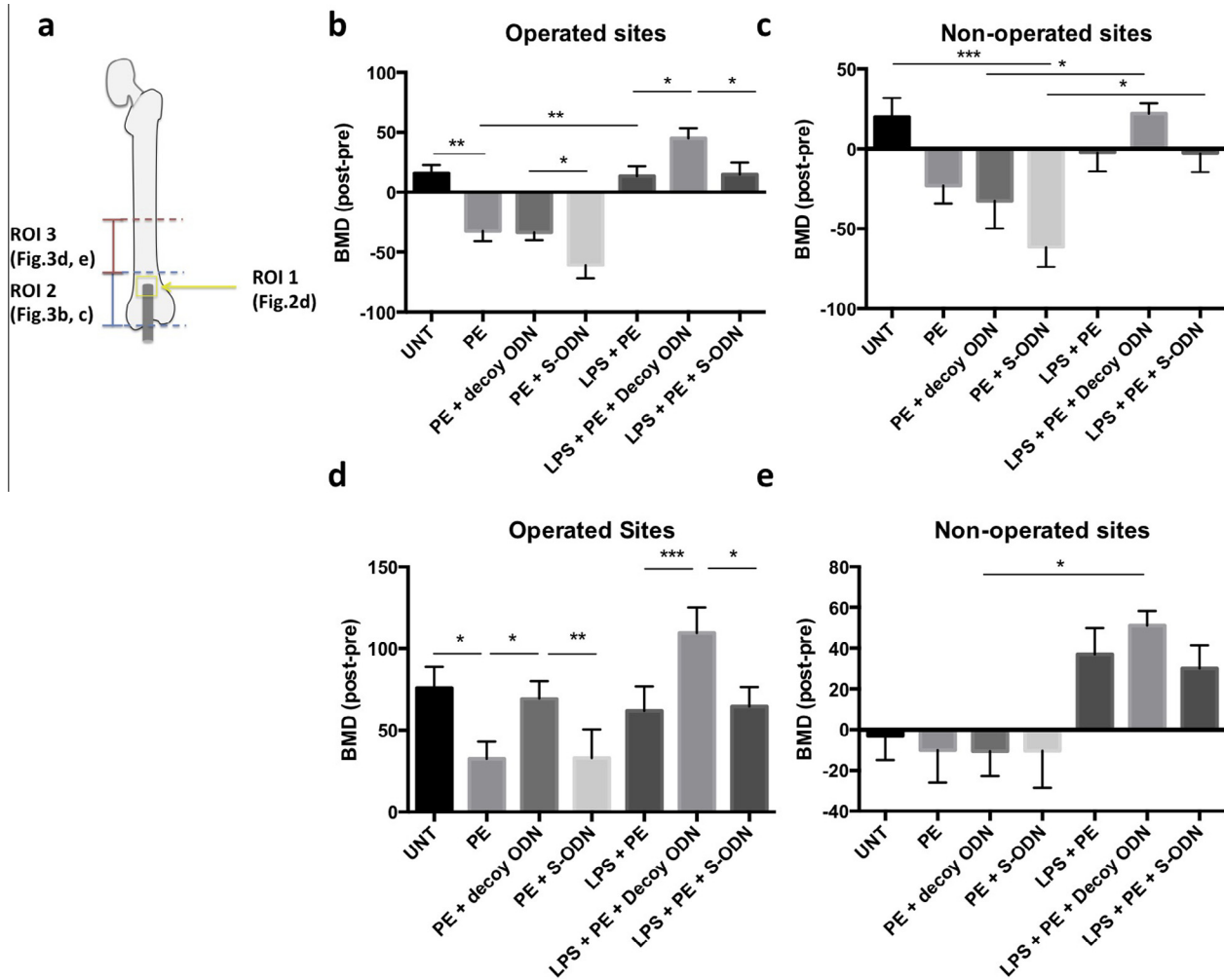
Fig. 3. NF-κB decoy ODN increased BMD in the confined region of bone exposed to UHMWPE particles with/without LPS. (a) Illustration of ROI 1–3 around distal end of femur. BMD in the ROI 2 & 3 ($4 \times 4 \times 3$ mm^3) was normalized by the pre-operation scan. ROI containing metaphysis region (ROI2, b–c) or diaphysis region (ROI3, d–e) at operated (b and d) or non-operated sites (c and e) were analyzed by MicroView Software. PE: UHMWPE particles; UNT: untreated control; S-ODN: scrambled ODN. *p < 0.05, **p < 0.01, ***p < 0.005.

3.5. NF-κB decoy ODN suppressed osteoclast numbers induced by UHMWPE wear particle with LPS and had no significant effect on osteoblast differentiation

The osteoclast number determined by TRAP staining (Fig. 5a and b) was increased in the group with particle infusion (8.53 ± 0.51 cells/0.01 mm^2) or combined with LPS (10.93 ± 1.19 cells/0.01 mm^2) compared to the untreated control group (2.94 ± 0.65 cells/0.01 m^2). Decoy ODN reduced TRAP+ cell number in particle alone group (5.60 ± 0.38 cells/0.01 mm^2) and particle plus LPS group (6.37 ± 0.62 cells/0.01 mm^2), but remained higher than the untreated control (p = 0.02 and 0.04, respectively). The TRAP+ cell numbers in scrambled ODN were comparable to the control groups with particle infusion alone (9.07 ± 0.71 cells/0.01 mm^2) or particle plus LPS (9.82 ± 0.63 cells/0.01 mm^2), respectively. The osteoblast number determined by ALP staining showed no significant difference among the groups (Fig. 5a and c). Decoy ODN treatment did not increase osteoblast numbers in the particle infusion alone group (6.26 ± 0.57 cells/100 μm) when compared with the untreated group (3.30 ± 0.34 cells/100 μm, p = 0.079).

4. Discussion

The current findings demonstrated that modulation of NF-κB activity via decoy ODN mitigated wear particle-associated bone loss in an in vivo clinically relevant murine continuous femoral particle infusion model. The numbers of infiltrated macrophages and activated osteoclasts were reduced by decoy ODN treatment, but there were no significant effects on osteoblast differentiation. Together with our previous in vitro and in vivo studies [8,12,13], we demonstrated that NF-κB is a highly potential therapeutic target for peri-prosthetic osteolysis.

Wear particle-induced inflammation and osteolysis around implants can result in aseptic loosening [4], and consequently lead to revision surgery in TJR patients. Our results demonstrated that NF-κB decoy ODN significantly reversed particle-induced trabecular bone loss around the implants (Fig. 2). However, detailed information of the bone-implant interface is limited in the current model, due to rod removal first prior to histological and mechanistic studies using frozen tissue sections. The strategic use of decoy ODN is highly specific, and directly inhibits the binding of NF-κB to the targeted genomic sequence. Also, local delivery of decoy ODN has the advantage of avoiding systemic side effects. In potential clinical application, NF-κB decoy ODN could be applied during the first several months after TJR to mitigate particle-induced inflammation, and possibly generate a more robust interface around the implants. In addition, the decoy ODN could also be applied at a later time in the early stages of periprosthetic osteolysis to mitigate the bone loss when the wear process continues [21]. The decoy ODN treatment reduced macrophage infiltration in the presence of LPS, which
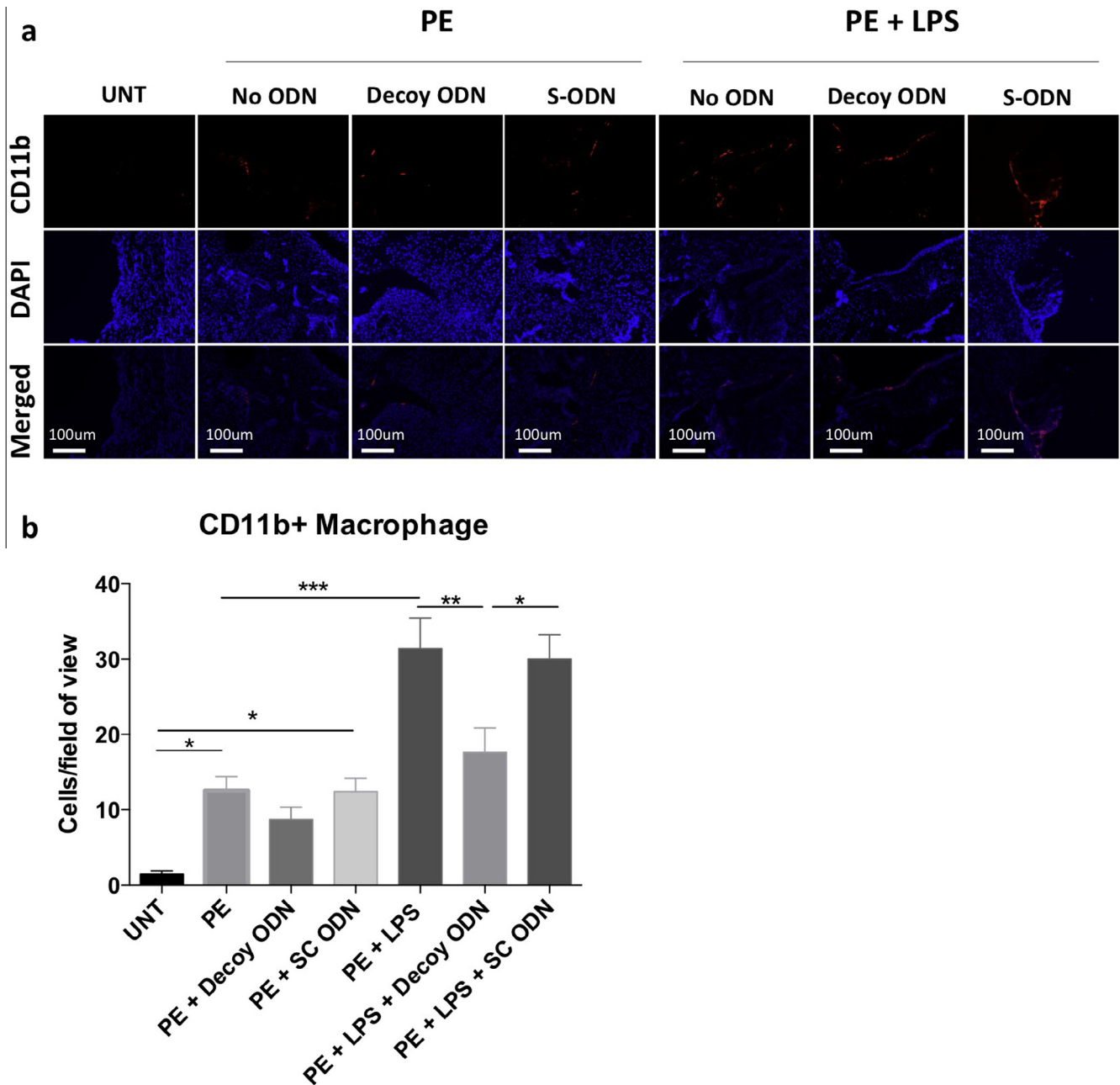
Fig. 4. NF-κB decoy ODN treatment reduced macrophage infiltration in the distal femur in response to UHMWPE particles with LPS. (a) CD11b (PE) and Cellular nucleus (DAPI) images were captured under fluorescence microscope. (b) CD11b positive cell numbers per image view were counted manually in 3 randomly selected views. PE: UHMWPE particles; UNT: untreated control; S-ODN: scrambled ODN. $^*p < 0.05$, $^{**}p < 0.01$, $^{***}p < 0.005$.

may impair the local innate immune response to bacterial infection. Therefore, combined treatment with antibiotic prophylaxis may be considered during decoy ODN treatment. Also, it should be noted that inflammation is an integral part of the healing process [22–24]. Manipulation of the pro-inflammatory response without interfering with the healing mechanisms is crucial for the osseointegration of implants.

Although the infusion of particles and LPS significantly decreased BVF in the confined region around the implants (Fig. 2), the BMD at the metaphyseal and diaphyseal regions were increased (Fig. 3). Although the pro-inflammatory response to particles and LPS can induce osteoclast activation, their effect on osteogenesis seems paradoxical [25–31]. The varying results reported in previous in vitro and in vivo studies could be the result

of the dose, exposure time, administration strategy, source of endotoxin, and cell types. In our current findings, it is likely that the primary effect of direct LPS exposure pushes the balance between osteoblastic and osteoclastic activity towards bone loss. The secondary pro-inflammatory mediators could potentially push the balance toward bone formation in both operated and non-operated sites (Fig. 3). *Staphylococcus aureus* and *Staphylococcus epidermidis* and lipoteichoic acid (LTA) could also be relevant as danger signal molecules adhering to the particles, as these bacteria are common pathogens in orthopaedic implant infections [32]. Notably, previous reports indicated that LTA treatment showed no effects on mesenchymal stem cells during osteogenesis [25,28]. These pathogen-associated molecular patterns can be recognized by cells through different TLRs. For example, LTA and
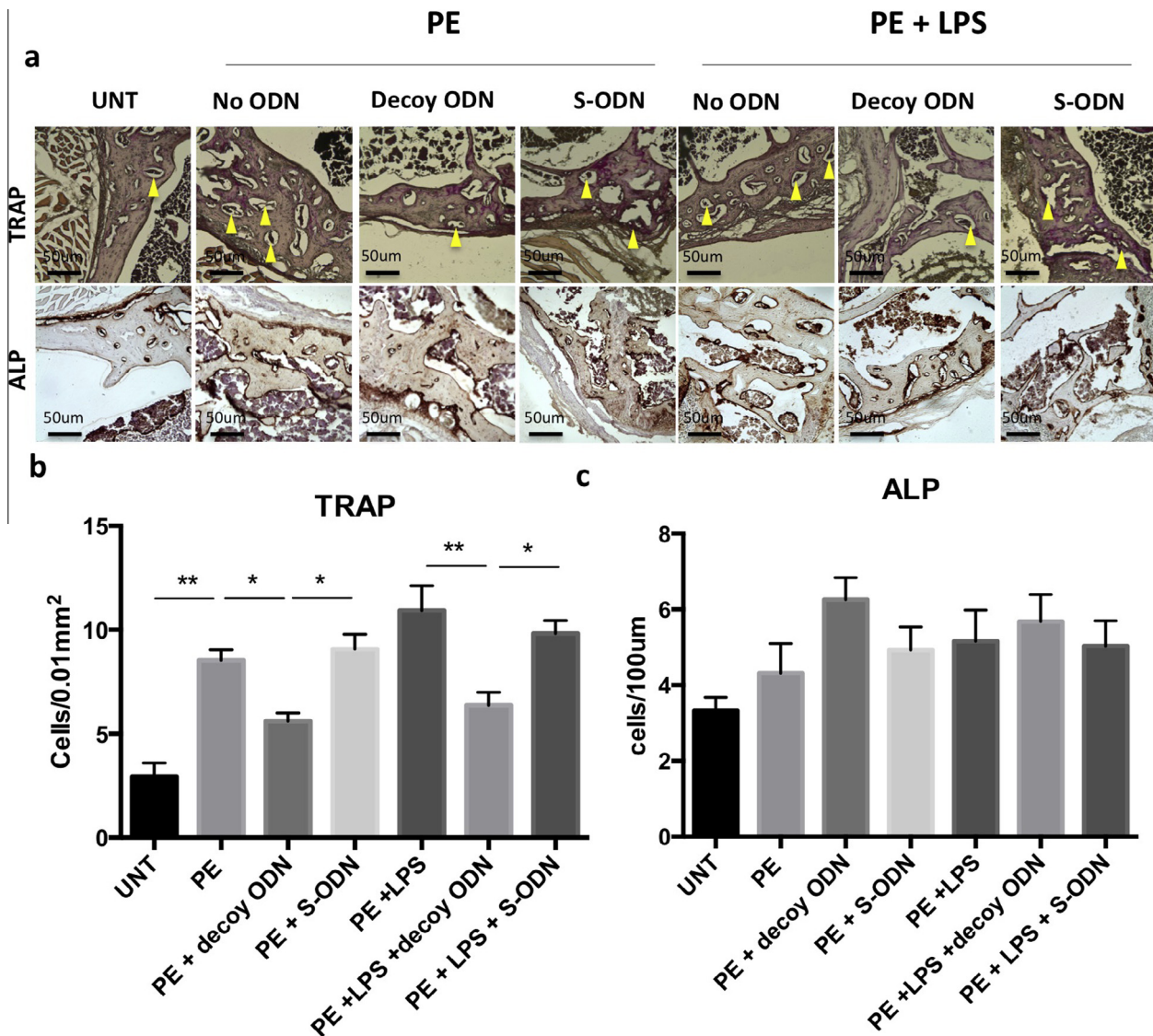
Fig. 5. NF-κB decoy ODN treatment reduced osteoclast activation, and has no significant effects on osteoblastic activity in the distal femur in response to UHMWPE particles with or without LPS. (a) TRAP staining was used to determine active osteoclast number (upper panel), and alkaline phosphatase (ALP) was used to determine osteoblast number (lower panel). The TRAP+ (b) and ALP+ (c) cell numbers were counted manually, and the numbers were normalized as described in Section 2. PE: UHMWPE particles; UNT: untreated control; S-ODN: scrambled ODN. $^*p < 0.05$, $^{**}p < 0.01$.

LPS can be recognized by TLR2 and TLR4 respectively. Activation of TLR2 or TLR4 signaling pathway may have distinct functions during osteogenesis.

The stability of ODN is one of the most challenging issues when applied to in vivo models, as the ODN could be degraded by abundant nucleases in serum and interstitial fluid [33]. Our in vitro pump-releasing model showed that the inhibition of TNF-α secretion by decoy ODN in the immortalized mouse monocyte/macrophage RAW264.7 cell line was not as clear as the suppression of NF-κB activity. The results suggested that other cellular signaling pathways might compensate for the induction of TNF-α during decoy ODN treatment [34]. Also, the decoy ODN remains functional for 4 weeks in a protected environment in the pumps, but then maybe less effective probably due to degradation of ODN into smaller molecules. Thus the development of advanced technologies would be essential to administer the decoy ODN for a longer period of time. Recent development of layer-by-layer coating or hydrogel-based long-term releasing technologies allows efficient loading and controlled release for the administration of protein or ODN-based therapy. Coating on the surface of implanted devices

has been used to administer proteins, small molecules, decoy ODN, or other potential therapeutic compounds [35–38]. Long-term release of drugs for up to 60 days can be achieved by controlling the mesh size and degradation rate in a polyethylene glycol (PEG) based hydrogel model [39]. These administration techniques could potentially further enhance the therapeutic efficiency of the decoy ODN in the clinical scenario.

We have previously demonstrated that naked decoy ODN was able to suppress NF-κB activity in macrophages and mesenchymal stem cells in vitro [8,12]. ODN could be taken up by the cells through a receptor-mediated pathway, which is sensitive to the sequence specificity [40]. This receptor-mediated mechanism allows ODN to escape from the degradation in the endolysosomal compartment and enter the cell nucleus. We noticed that the scrambled ODN decreased bone mineral density at the metaphysis in both operated and non-operated femurs (Fig. 3b and c). It is likely that the sequence of scrambled ODN may have lower affinity to cellular receptors and therefore have a higher chance to activate TLR9 during the endocytosis process [41]. The resultant inflammation may induce bone loss through paracrine effects at the metaphysis,

and the effects could be masked in the presence of overwhelming inflammatory stimuli such as LPS. In the tissue microenvironment exposed to ODNs, macrophages could take up the ODN via Mac-1 (also known as CD11b, a macrophage specific cell surface receptor) [42]. It remains unclear that if there is a potential cellular receptor that could mediate ODN uptake by other cell types such as osteoblasts or osteoclasts. The strategic use of fluorescence dye labeled ODN could potentially identify specific cellular targets of NF-κB decoy ODN based therapy in future experiments [43].

5. Conclusion

Administration of NF-κB decoy ODN mitigated UHMWPE wear particle and endotoxin-induced inflammatory bone loss in vivo. Local delivery of NF-κB ODN could potentially reduce periprosthetic osteolysis and the revision rate due to wear particles from joint replacements.

Acknowledgements

References

[1] A. Tsao, L. Jones, D. Lewallen, Implant Wear Symposium Clinical Work G. What patient and surgical factors contribute to implant wear and osteolysis in total joint arthroplasty?, J Am. Acad. Orthop. Surg. 16 (Suppl 1) (2008) 13.

[2] P. Purdue, P. Koulouvaris, B. Nestor, T. Sculco, The central role of wear debris in periprosthetic osteolysis, HSS J.: Musculoskeletal Journal of Hospital for Special Surgery 2 (2006) 102–113.

[3] E.M. Greenfield, Do genetic susceptibility, Toll-like receptors, and pathogen-associated molecular patterns modulate the effects of wear?, Clin Orthop. Relat. Res. 472 (2014) 3709–3717.

[4] J. Pajarinen, E. Jamsen, Y.T. Konttinen, S.B. Goodman, Innate immune reactions in septic and aseptic osteolysis around hip implants, J. Long Term Eff. Med. Implants 24 (2014) 283–296.

[5] J.I. Pearl, T. Ma, A.R. Irani, Z. Huang, W.H. Robinson, R.L. Smith, et al., Role of the Toll-like receptor pathway in the recognition of orthopedic implant wear-debris particles, Biomaterials 32 (2011) 5535–5542.

[6] Y. Nakashima, D. Sun, M. Trindade, W. Maloney, S. Goodman, D. Schurman, et al., Signaling pathways for tumor necrosis factor-alpha and interleukin-6 expression in human macrophages exposed to titanium-alloy particulate debris in vitro, J. Bone Joint Surg. Am. 81 (1999) 603–615.

[7] A.J. Rao, E. Gibon, T. Ma, Z. Yao, R.L. Smith, S.B. Goodman, Revision joint replacement, wear particles, and macrophage polarization, Acta Biomater. 8 (2012) 2815–2823.

[8] T.H. Lin, T. Sato, K.R. Barcay, H. Waters, F. Loi, R. Zhang, et al., NF-kappaB decoy oligodeoxynucleotide enhanced osteogenesis in mesenchymal stem cells exposed to polyethylene particle, Tissue Eng. Part A (2014).

[9] T.H. Lin, Y. Tamaki, J. Pajarinen, H.A. Waters, D.K. Woo, Z. Yao, et al., Chronic inflammation in biomaterial-induced periprosthetic osteolysis: NF-kappaB as a therapeutic target, Acta Biomater. 10 (2014) 1–10.

[10] M.A. Calzado, S. Bacher, M.L. Schmitz, NF-kappaB inhibitors for the treatment of inflammatory diseases and cancer, Curr. Med. Chem. 14 (2007) 367–376.

[11] M. Osako, H. Nakagami, R. Morishita, Modification of decoy oligodeoxynucleotides to achieve the stability and therapeutic efficacy, Curr. Top. Med. Chem. 12 (2012) 1603–1607.

[12] T.H. Lin, Y. Tamaki, T. Sato, M. Keeney, C. Li, J. Pajarinen, et al., Suppression of wear-particle-induced pro-inflammatory cytokine and chemokine production in macrophages via NF-kappaB decoy oligodeoxynucleotide: a preliminary report, Acta Biomater. 10 (2014) 3747–3755.

[13] T. Sato, J. Pajarinen, T.H. Lin, Y. Tamaki, F. Loi, Z. Yao, et al., NF-kappaB decoy oligodeoxynucleotide inhibits wear particle-induced inflammation in a murine calvarial model, J. Biomed. Mater. Res., Part A (2015).

[14] S. Khosla, Minireview: the OPG/RANKL/RANK system, Endocrinology 142 (2001) 5050–5055.

[15] P.G. Ren, A. Irani, Z. Huang, T. Ma, S. Biswal, S.B. Goodman, Continuous infusion of UHMWPE particles induces increased bone macrophages and osteolysis, Clin. Orthop. Relat. Res. 469 (2011) 113–122.

[16] H. Shimizu, H. Nakagami, S. Morita, I. Tsukamoto, M. Osako, F. Nakagami, et al., New treatment of periodontal diseases by using NF-kappaB decoy oligodeoxynucleotides via prevention of bone resorption and promotion of wound healing, Antioxid. Redox Signal. 11 (2009) 2065–2075.

[17] P. Campbell, S. Ma, B. Yeom, H. McKellop, T. Schmalzried, H. Amstutz, Isolation of predominantly submicron-sized UHMWPE wear particles from periprosthetic tissues, J. Biomed. Mater. Res. 29 (1995) 127–131.

[18] J. Pajarinen, Y. Tamaki, J.K. Antonios, T.H. Lin, T. Sato, Z. Yao, et al., Modulation of mouse macrophage polarization in vitro using IL-4 delivery by osmotic pumps, J. Biomed. Mater. Res., Part A (2014).

[19] A. Xagorari, C. Roussos, A. Papapetropoulos, Inhibition of LPS-stimulated pathways in macrophages by the flavonoid luteolin, Br. J. Pharmacol. 136 (2002) 1058–1064.

[20] E. Gibon, Z. Yao, A.J. Rao, S. Zwingenberger, B. Batke, R. Valladares, et al., Effect of a CCR1 receptor antagonist on systemic trafficking of MSCs and polyethylene particle-associated bone loss, Biomaterials 33 (2012) 3632–3638.

[21] D.H. Sochart, Relationship of acetabular wear to osteolysis and loosening in total hip arthroplasty, Clin. Orthop. Relat. Res. (1999) 135–150.

[22] K.A. Alexander, M.K. Chang, E.R. Maylin, T. Kohler, R. Muller, A.C. Wu, et al., Osteal macrophages promote in vivo intramembranous bone healing in a mouse tibial injury model, J. Bone Miner. Res.: The official journal of the American Society for Bone and Mineral Research 26 (2011) 1517–1532.

[23] P. Guihard, Y. Danger, B. Brounais, E. David, R. Brion, J. Delecrin, et al., Induction of osteogenesis in mesenchymal stem cells by activated monocytes/macrophages depends on oncostatin M signaling, Stem cells 30 (2012) 762–772.

[24] O.M. Omar, C. Graneli, K. Ekstrom, C. Karlsson, A. Johansson, J. Lausmaa, et al., The stimulation of an osteogenic response by classical monocyte activation, Biomaterials 32 (2011) 8190–8204.

[25] I.F. Mo, K.H. Yip, W.K. Chan, H.K. Law, Y.L. Lau, G.C. Chan, Prolonged exposure to bacterial toxins downregulated expression of toll-like receptors in mesenchymal stromal cell-derived osteoprogenitors, BMC Cell Biol. 9 (2008) 52.

[26] M. Croes, F.C. Oner, M.C. Kruyt, T.J. Blokhuis, O. Bastian, W.J. Dhert, et al., Proinflammatory mediators enhance the osteogenesis of human mesenchymal stem cells after lineage commitment, PLoS ONE 10 (2015) e0132781.

[27] C. Li, B. Li, Z. Dong, L. Gao, X. He, L. Liao, Lipopolysaccharide differentially affects the osteogenic differentiation of periodontal ligament stem cells and bone marrow mesenchymal stem cells through Toll-like receptor 4 mediated nuclear factor kappaB pathway, Stem Cell Res. Ther. 5 (2014) 67.

[28] T. Fiedler, A. Salamon, S. Adam, N. Herzmann, J. Taubenheim, K. Peters, Impact of bacteria and bacterial components on osteogenic and adipogenic differentiation of adipose-derived mesenchymal stem cells, Exp. Cell Res. 319 (2013) 2883–2892.

[29] L.A. Bonsignore, J.R. Anderson, Z. Lee, V.M. Goldberg, E.M. Greenfield, Adherent lipopolysaccharide inhibits the osseointegration of orthopedic implants by impairing osteoblast differentiation, Bone 52 (2013) 93–101.

[30] K. Bandow, A. Maeda, K. Kakimoto, J. Kusuyama, M. Shamoto, T. Ohnishi, et al., Molecular mechanisms of the inhibitory effect of lipopolysaccharide (LPS) on osteoblast differentiation, Biochem. Biophys. Res. Commun. 402 (2010) 755–761.

[31] N. Tomomatsu, K. Aoki, N. Alles, N.S. Soysa, A. Hussain, H. Nakachi, et al., LPS-induced inhibition of osteogenesis is TNF-alpha dependent in a murine tooth extraction model, J. Bone Miner. Res.: The official journal of the American Society for Bone and Mineral Research 24 (2009) 1770–1781.

[32] A. Trampuz, W. Zimmerli, New strategies for the treatment of infections associated with prosthetic joints, Curr. Opin. Investig. Drugs 6 (2005) 185–190.

[33] M.K. Osako, H. Nakagami, R. Morishita, Modification of decoy oligodeoxynucleotides to achieve the stability and therapeutic efficacy, Curr. Top. Med. Chem. 12 (2012) 1603–1607.

[34] J.K. Kim, S.M. Lee, K. Suk, W.H. Lee, A novel pathway responsible for lipopolysaccharide-induced translational regulation of TNF-alpha and IL-6 expression involves protein kinase C and fascin, J. Immunol. 187 (2011) 6327–6334.

[35] M. Keeney, H. Waters, K. Barcay, X. Jiang, Z. Yao, J. Pajarinen, et al., Mutant MCP-1 protein delivery from layer-by-layer coatings on orthopedic implants to modulate inflammatory response, Biomaterials 34 (2013) 10287–10295.

[36] S.B. Goodman, Z. Yao, M. Keeney, F. Yang, The future of biologic coatings for orthopaedic implants, Biomaterials 34 (2013) 3174–3183.

[37] Y. Hu, H.-f. Wang, W.-q. Sun, C.-s. Xie, W.-n. Wei, J.-e. Zheng, et al., Regulation of tissue factor expression in brain microvascular endothelial cells by PLA nanoparticles coating NF-kappaB decoy oligonucleotides, Zhonghua xue ye xue za zhi = Zhonghua xueyexue zazhi 26 (2005) 534–538.

[38] M. Kalinowski, K. Viehofer, C. Hamann, J. Barry, B. Kleb, K. Klose, et al., Local administration of NF-kappa B decoy oligonucleotides to prevent restenosis after balloon angioplasty: an experimental study in New Zealand white rabbits, Cardiovasc. Intervent. Radiol. 28 (2005) 331–337.

[39] X. Tong, S. Lee, L. Bararpour, F. Yang, Long-term controlled protein release from poly(ethylene glycol) hydrogels by modulating mesh size and degradation, Macromol. Biosci. (2015).

[40] R.L. Juliano, X. Ming, O. Nakagawa, Cellular uptake and intracellular trafficking of antisense and siRNA oligonucleotides, Bioconjug. Chem. 23 (2012) 147–157.

[41] R. Fukui, K. Miyake, Controlling systems of nucleic acid sensing-TLRs restrict homeostatic inflammation, Exp. Cell Res. 318 (2012) 1461–1466.

[42] L. Benimetskaya, J.D. Loike, Z. Khaled, G. Loike, S.C. Silverstein, L. Cao, et al., Mac-1 (CD11b/CD18) is an oligodeoxynucleotide-binding protein, Nat. Med. 3 (1997) 414–420.

[43] M. Miteva, K.C. Kirkbride, K.V. Kilchrist, T.A. Werfel, H. Li, C.E. Nelson, et al., Tuning PEGylation of mixed micelles to overcome intracellular and systemic siRNA delivery barriers, Biomaterials 38 (2015) 97–107.